Available online at www.sciencedirect.com
SCIENCE DIRECT®
Journal of Solid State Chemistry 178 (2005) 1569–1574
JOURNAL OF SOLID STATE CHEMISTRY
www.elsevier.com/locate/jssc

Synthesis, crystal structure and properties of $K_2Ta_2S_{10}$: A novel ternary tantalum polysulfide with TaS_8 polyhedra forming infinite anionic chains

Yuandong Wu, Christian Näther, Wolfgang Bensch*

Institut für Anorganische Chemie, Christian-Albrechts-Universität Kiel, Arbeitskreis Bensch, Olshausenstr. 40 (Otto-Hahn-Platz 7), D-24108 Kiel, Germany

Received 17 November 2004; received in revised form 17 November 2004; accepted 13 February 2005

Abstract

The new ternary alkali tantalum polysulfide $K_2Ta_2S_{10}$ has been synthesized by reacting TaS_2 with an in situ formed melt of K_2S_3 and S at 773 K. The compound crystallizes with four formula units in the monoclinic space group $P2_1/n$ (No. 14) with lattice parameters of $a = 14.9989(13)$ Å, $b = 6.4183(4)$ Å, $c = 15.1365(13)$ Å, $\beta = 117.629(9)°$. The structure contains two different zigzag chain anions $[TaS_5]^-$, running parallel to the crystallographic *b*-axis separated by potassium cations. The two crystallographically independent tantalum atoms are in a distorted bi-capped trigonal prismatic environment of eight sulfur atoms which was never observed before. The TaS_8 polyhedra share three S atoms on each side to form the anionic chains. The compound was characterized with FIR and Raman spectroscopy.

Keywords: Ternary tantalum sulfide; Crystal structure; IR; Raman spectrum

1. Introduction

The so-called reactive molten flux method [1–3] employing alkali metal polychalcogenides is a powerful tool to synthesize novel compounds at temperatures between 523 and 773 K. The products are often obtained as well developed single crystals that enable unambiguous characterization by single crystal X-ray diffraction. Due to the relatively low reaction temperature compounds containing large $Q_x{}^{2-}$ anions are accessible which cannot be obtained by "classical" high-temperature syntheses. Recently, a large number of ternary group 5 chalcogenide compounds with a variety of metal cations including alkali metals has been reported. Depending on the reaction conditions and size of the cations, structures with discrete molecular anions [4–20] or chains [21–24] are formed. In the case of tantalum, examples include discrete tetrahedral TaQ_4 units like in A_3TaQ_4 (A = K, Rb, Cs, Q = S, Se) [6–8], Ta_2S_{11} groups like in $A_4Ta_2S_{11}$ (A = K, Rb, Cs) [13–15], complex Ta_4S_{22} units like in $A_6Ta_4S_{22}$ (A = K, Rb, Cs) [16,18,19], and Ta_4S_{25} like in $Rb_6Ta_4S_{25}$ units [20]. The Ta_2S_{11} unit is composed of two face sharing TaS_7 pentagonal bipyramids and is a building block which may be interconnected through S_2^{2-} and S_5^{2-} polyanions yielding the Ta_4S_{22} and Ta_4S_{25} unit. Anionic chains are observed in $ATaQ_3$ (A = K, Cs, Q = S, Se, Te) [21,23] and in $K_{12}Ta_6Se_{35}$ [23]. The anionic $[TaQ_3]^-$ chains are composed of face-sharing TaS_6 octahedra in which the Ta^{5+} ions are displaced from the centers of the octahedra along the direction of the chains in a pair-wise fashion. In $K_{12}Ta_6Se_{35}$ the anionic chains are arranged in layers parallel to the (010)-plane and successive planes are rotated by 33° against each other. The Ta_2Se_{11} units are interconnected by Se_2^{2-} and Se_3^{2-} polyanions forming infinite ${}^1_\infty[Ta_6Se_{35}]^{12-}$ chains.

*Corresponding author. Fax: +49 4341 880 1520.
E-mail address: wbensch@ac.uni-kiel.de (W. Bensch).

0022-4596/$ - see front matter
doi:10.1016/j.jssc.2005.02.010

In this paper, we report on the synthesis and characterization of the new ternary tantalum sulfide compound $K_2Ta_2S_{10}$. To the best of our knowledge this compound has not been reported until now. It is the first ternary tantalum polysulfide exhibiting ${}^1_\infty[TaS_5]^-$ anionic chains built up by $[Ta(S_2)_2(S)_4]$ groups sharing faces through S_2 and S_{22} anions.

2. Experimental

2.1. Synthesis

The compound $K_2Ta_2S_{10}$ was prepared by reacting a mixture of K_2S_3 (0.0927 g, 0.53 mmol), TaS_2 (0.1734 g, 0.75 mmol), and S powder (0.0344 g, 1.06 mmol) in a 3:4:6 molar ratio. K_2S_3 was synthesized by the reaction of stoichiometric amounts of the elements (K, >99%, Chempur; S, 99.99%, Heraeus) in liquid ammonia under argon atmosphere. The starting material TaS_2 was prepared by heating stoichiometric amounts of the elements (Ta, 99.97%, Fluka) at 1123 K in an evacuated silica tube. The starting material was thoroughly mixed in a N_2-filled glove box and loaded into a Pyrex glass ampoule. After evacuation to 10^{-3} mbar the ampoule was flame-sealed and placed in a computer-controlled furnace. The ampoule was heated to 773 K at a rate of 30 K h^{-1}, kept at this temperature for 6 days, followed by a cooling to 373 K with 2 K h^{-1} and a rapid cooling to room temperature. The solid products were washed with DMF and acetone to remove residual polysulfide flux. The reaction product consists of a mixture of dark red needles of $K_2Ta_2S_{10}$ (yield: ~60% based on Ta) and orange-yellow polyhedra (yield: ~40%), which were identified as $K_6Ta_4S_{22}$ by single crystal X-ray diffraction. The new polysulfide $K_2Ta_2S_{10}$ is stable in dry air for several weeks. The X-ray powder pattern of the dark red needles could successfully be refined on the basis of the lattice parameters of $K_2Ta_2S_{10}$. An EDX analysis indicated the presence of all three elements (K, Ta, S) in an approximate atomic ratio of 1:1:5.3 which is in good agreement with the composition derived from the crystallographic structure determination.

2.2. Crystallography

Data collection was performed on a STOE Imaging Plate Diffraction System (IPDS) (Mo$K\alpha$ radiation; $\lambda = 0.71073$ Å) equipped with a low-temperature device from Oxford Cryosystems at 180 K. The raw intensities were treated in the usual way applying a Lorentz, polarization and a numerical absorption correction. Structure solution was performed with SHELXS-97 [25]. Refinement was done against F^2 using SHELXL-97 [26]. All atoms were refined with anisotropic displacement parameters. Technical details of the data acquisition as well as some refinement results are summarized in Table 1, atomic coordinates and equivalent isotropic displacement parameters are given in Table 2. Selected bond distances are listed in Table 3.

Further details of the crystal structure investigation can be obtained from the Fachinformationszentrum Karlsruhe, 76344 Eggenstein-Leopoldshafen, Germany (fax: (49) 7247 808 666; E-mail: crysdata@fiz-karlsruhe.de) on quoting the depository number CSD-414535.

2.3. Optical property measurements

A Far-IR spectrum was recorded between 80 and 550 cm^{-1} (resolution = 2 cm^{-1}) on an ISF-66 device (Bruker) with $K_2Ta_2S_{10}$ pressed in polyethylen pellets. The FT-Raman spectrum was measured on an ISF-66 spectrometer (Bruker) with an additional FRA 106 Raman modul. A Nd/YAG laser was used as source for excitation ($\lambda = 1064$ nm). $K_2Ta_2S_{10}$ was ground and

Table 1
Technical details of data acquisition and some refinement results for $K_2Ta_2S_{10}$

Empirical formula	$K_2Ta_2S_{10}$
Formula weight/g/mol	760.80
Temperature	180 K
Wavelength/Å	0.71073
Crystal system	Monoclinic
Space group	$P2_1/n$
a/Å	14.9989(13)
b/Å	6.4183(4)
c/Å	15.1365(13)
β/°	117.629(9)
V/Å^3	1290.99(18)
Z	4
Calculated density/g cm^{-3}	3.914
Crystal color	Dark red
μ/mm^{-1}	19.154
$F(000)$	1376
Crystal size/mm^3	0.13 × 0.11 × 0.095
θ range	2.61–27.93°
Index range	$-19 \leqslant h \leqslant 19$
	$-7 \leqslant k \leqslant 8$
	$-19 \leqslant l \leqslant 19$
Reflections collected	12035
Independent reflections	3035
R_{int}	0.0257
Completeness to $\theta = 27.93°$	97.9%
Refinement method	Full-matrix least square on F^2
Min./max. transm.	0.095/0.162
Refl. with $F_o > 4\sigma(F_o)$	2796
Number of parameters	128
Goodness-of-fit on F^2	1.033
Final R indices ($F_o > 4\sigma(F_o)$)[a,b]	$R1 = 0.0220$, w$R2 = 0.0550$
R indices (all data)[a,b]	$R1 = 0.0247$, w$R2 = 0.0561$
Extinction coefficient	0.00123(9)
Largest diff. peak and hole/e Å^{-3}	1.626/−2.426

[a] $R1 = \Sigma||F_o|-|F_c||/\Sigma|F_o|$.
[b] $wR2 = [\Sigma w(F_o^2-F_c^2)^2/\Sigma w(F_o^2)^2]^{1/2}$, $w = 1/[\sigma(F_o^2)+(aP)^2+bP]$, where $P = (\max(F_o^2,0)+2\cdot F_c^2)/3$.

Table 2
Atomic coordinates and equivalent isotropic displacement parameters U_{eq} ($Å^2 \times 10^3$) for $K_2Ta_2S_{10}$

	x	y	z	U_{eq}
Ta(1)	0.2436(1)	0.5803(1)	0.2081(1)	6(1)
Ta(2)	0.2047(1)	0.4506(1)	−0.2563(1)	6(1)
K(1)	0.4360(1)	0.3538(2)	0.0857(1)	18(1)
K(2)	0.0850(1)	−0.1408(2)	−0.0680(1)	19(1)
S(1)	0.2395(1)	0.2427(2)	0.1251(1)	9(1)
S(2)	0.1201(1)	0.8648(2)	0.1637(1)	9(1)
S(3)	0.3339(1)	0.6673(2)	−0.1206(1)	9(1)
S(4)	0.3781(1)	0.2883(2)	−0.2344(1)	10(1)
S(5)	0.1232(1)	0.3534(2)	0.2525(1)	9(1)
S(6)	0.2454(1)	0.1780(2)	−0.1249(1)	9(1)
S(7)	0.3103(1)	0.7405(2)	0.1020(1)	10(1)
S(8)	0.0514(1)	0.6098(2)	−0.3937(1)	11(1)
S(9)	0.1082(1)	0.4146(2)	0.0530(1)	11(1)
S(10)	0.0997(1)	0.3012(2)	−0.1903(1)	12(1)

Estimated standards deviations are given in parentheses. The U_{eq} is defined as one third of the trace of the orthogonalized U_{ij} tensors.

Table 3
Selected bond distances (Å) for $K_2Ta_2S_{10}$

Ta(1)–S(1)	2.4906(11)	Ta(1)–S(1)	2.6327(11)
Ta(1)–S(2)	2.4628(11)	Ta(1)–S(2)	2.4853(11)
Ta(1)–S(5)	2.5130(11)	Ta(1)–S(5)	2.6385(11)
Ta(1)–S(7)	2.4753(11)	Ta(1)–S(9)	2.5191(11)
Ta(2)–S(3)	2.4680(11)	Ta(2)–S(3)	2.4779(11)
Ta(2)–S(4)	2.4680(11)	Ta(2)–S(4)	2.6389(11)
Ta(2)–S(6)	2.5089(11)	Ta(2)–S(6)	2.6541(11)
Ta(2)–S(8)	2.5165(11)	Ta(2)–S(10)	2.4545(11)
S(1)–S(9)	2.0717(15)	S(4)–S(8)	2.0707(15)
S(5)–S(7)	2.0818(15)	S(6)–S(10)	2.0911(15)
K(1)–S(1)	3.3443(15)	K(1)–S(3)	3.2425(15)
K(1)–S(3)	3.4219(16)	K(1)–S(4)	3.5069(16)
K(1)–S(6)	3.3400(15)	K(1)–S(8)	3.3828(16)
K(1)–S(8)	3.3830(15)	K(1)–S(7)	3.1947(15)
K(1)–S(10)	3.2851(16)	K(2)–S(1)	3.7001(16)
K(2)–S(2)	3.2506(15)	K(2)–S(2)	3.2959(15)
K(2)–S(4)	3.3153(15)	K(2)–S(5)	3.3646(15)
K(2)–S(6)	3.5545(15)	K(2)–S(7)	3.2495(15)
K(2)–S(9)	3.3202(16)	K(2)–S(9)	3.4857(16)
K(2)–S(10)	3.4504(16)		

prepared on Al sample holders. The measuring range was 100–3000 cm^{-1} with a resolution of 2 cm^{-1}. Resonance Raman spectra were measured on a multichannel Spectrometer XY (Dilor), excitation was obtained through Ar^+ and Kr^+ lasers (< 150 mW) at about 10 K.

UV/Vis/near-IR spectroscopic investigations were conducted at room temperature using a UV–VIS–NIR two-channel spectrometer Cary 5 from Varian Techtron Pty., Darmstadt. The compound was ground with KBr in a N_2-filled glove box and pressed into a transparent pellet. The UV/Vis/near-IR absorption spectrum was corrected for the scattering background.

3. Results and discussions

3.1. Crystal structure

The new tantalum polysulfide $K_2Ta_2S_{10}$ crystallizes in the monoclinic space group $P2_1/n$ (conventional setting: $P2_1/c$) with two unique K atoms, two crystallographically independent Ta atoms and ten crystallographically independent S atoms all of them located in general positions. In the structure of $K_2Ta_2S_{10}$ two different infinite $^1_\infty[TaS_5]^-$ chains running parallel to [010] are separated by the K^+ cations (Fig. 1). The shortest interchain S–S distance of 4.08 Å is much larger than the sum of van der Waals radii of S (3.6 Å). Each chain is surrounded by six other chains in a pseudo-hexagonal fashion. The two unique Ta atoms are in an eightfold coordination of S atoms. The resulting polyhedron may be described as a strong distorted bi-capped trigonal prism. Two rectangular faces are capped by S atoms of the S_2^{2-} anions (Fig. 2). We note that such a coordination environment was never observed before for Ta atoms. The Ta–S distances range from 2.463(1) to 2.639(1) Å with an average ⟨Ta–S⟩ of 2.527(1) Å for Ta(1) and from 2.455(1) to 2.654(1) Å (average ⟨Ta–S⟩: 2.526(1) Å) for Ta(2) (Table 3). These distances are in good agreement with the values reported for other potassium tantalum sulfides [13,14,16] and the sum of ionic radii of Ta and S as well [27].

The TaS_8 polyhedra share three S atoms on each side to form the one-dimensional chains, i.e. two edges of neighbored TaS_8 prisms and two S atoms which belong to one of the S_2^{2-} anions. All S_2^{2-} ions are bound to the Ta atoms in a μ_2-$\eta^1\eta^2$ mode whereas the S atoms connect the Ta atoms in a μ_2-bridging mode (Fig. 3). The description of the coordination mode of the compound is $K_2[Ta(1)(\mu_2\text{-}\eta^1\eta^2\text{-}S_2)_2(\mu_2\text{–}S)\ Ta(2)(\mu_2\text{-}\eta^1\eta^2\text{-}S_2)_2(\mu_2\text{–}S)]$ and the assignment of the formal valences is K^+, Ta^{5+}, S_2^{2-} and S^{2-}.

The chains propagate in a zigzag fashion as is evidenced by angle Ta–Ta–Ta of 139.3° for the chain

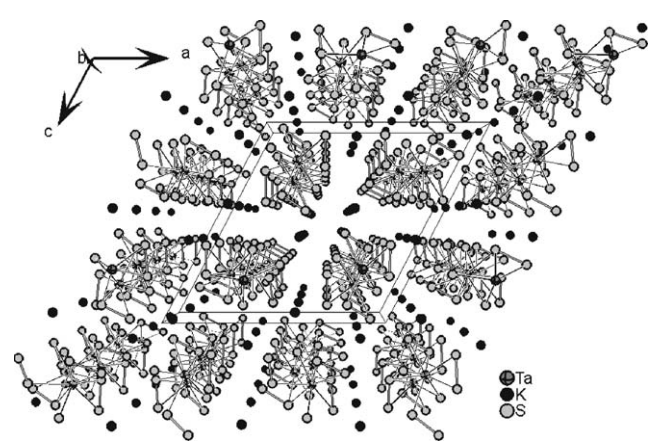

Fig. 1. Crystal structure of $K_2Ta_2S_{10}$ with view along [010].

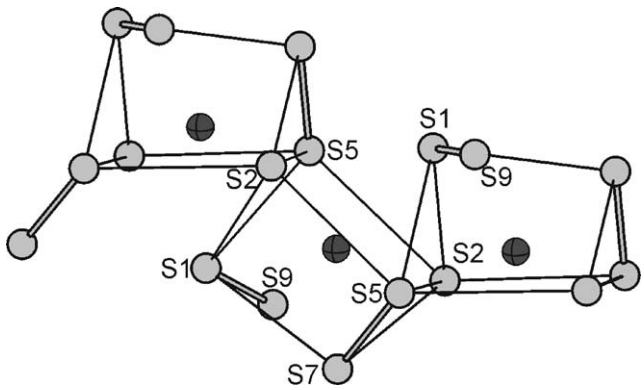

Fig. 2. The interconnection of the trigonal prisms via common edges. *Note*: the prisms are bi-capped with S1 and S9 being the capping atoms; the environment and interconnection around Ta(2) is very similar.

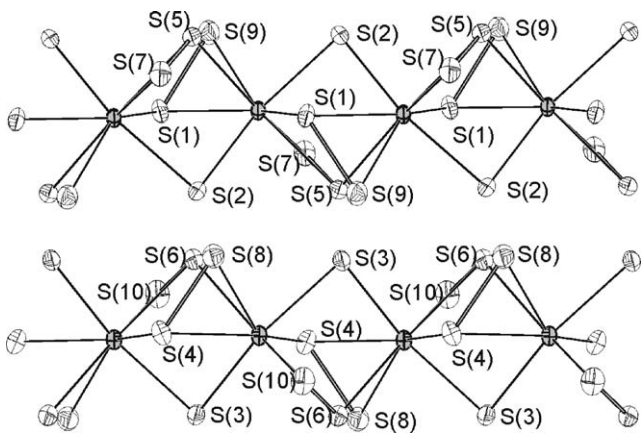

Fig. 3. Connection of TaS_5 polyhedra into chains for Ta1 (top) and Ta2 (bottom) (displacement ellipsoids are drawn at 90% probability level).

containing Ta(1) atoms and 140.0° for chains with the Ta(2) atoms. The Ta(1)–Ta(1) and Ta(2)–Ta(2) distances of 3.432(1) and 3.426(1) Å in the two distinct chains are about 0.7 Å longer than in metallic Ta (2.86 Å), too long for Ta–Ta interactions. The S–S bond lengths in the S_2^{2-} dumbbells range from 2.071(2) to 2.091(2) Å, and are in the usual range.

The two crystallographically distinct potassium atoms are in an irregular environment of nine S atoms with the K–S distances ranging from 3.195(2) to 3.507(2) Å (mean value: 3.345(2) Å) for K(1) and 3.250(2)–3.555(2) Å (mean value: 3.365(2) Å) for K(2), if a cutoff of 3.6 Å was chosen. For K(1) the S atoms are from two $[Ta(2)S_5]^-$ and one $[Ta(1)S_5]^-$ chains, and for K(2) from two $[Ta(1)S_5]^-$ and one $[Ta(2)S_5]^-$ chains. The average distances agree well with the sum of the ionic radii of K^+ (1.33 Å) and S^{2-} (1.84 Å) [27].

The structure of $K_2Ta_2S_{10}$ exhibits several similarities to that of $NaNbS_6$ [24]. In both structures the MS_x polyhedra are joined to form one-dimensional anionic zigzag chains. The S_2^{2-} anions are coordinated to two M^{5+} centers in the same μ_2-$\eta^1\eta^2$ mode. The main difference is the coordination number of the M^{5+} ions in the two compounds. In $NaNbS_6$ the Nb atom is surrounded by nine S atoms in an unusual $Nb(S_2)_3(S)_3$ coordination. The distorted tri-capped trigonal NbS_9 prisms are linked through three S atoms. Each corner of the trigonal prism is occupied by a S atom of a S_2^{2-} dumbbell. The environment of Nb is completed by three S atoms of S_2^{2-} anions which cap the rectangular faces of the distorted trigonal prisms. In contrast, in $K_2Ta_2S_{10}$ the Ta^{5+} ions are coordinated by eight S atoms forming the unusual $Ta(S_2)_2(S)_4$ polyhedron. In the title compound only three corners of the distorted trigonal TaS_8 prisms are occupied by S atoms of S_2 dumbbells. One S_2^{2-} anion forms the edge of one triangle of the prism and one S atom of the other S_2^{2-} anion is a capping atom.

3.2. Spectroscopy

The far-IR spectrum of $K_2Ta_2S_{10}$ displays absorptions at about 350 (s), 303 (s), 280 (vs), 238 (s), 195 (s), 174 (vw), 139 (vw), 115 (w) cm^{-1}. It is in good agreement with the Raman spectra, shown in Fig. 4 in the spectral range of 100–550 cm^{-1}. Due to the resonance Raman effect, the Raman spectra display significant dependencies on the excitation frequency. With the Nd–YAG laser excitation line (1064 nm), which is far away from the first electronic absorption band at 739 nm (Fig. 5), a

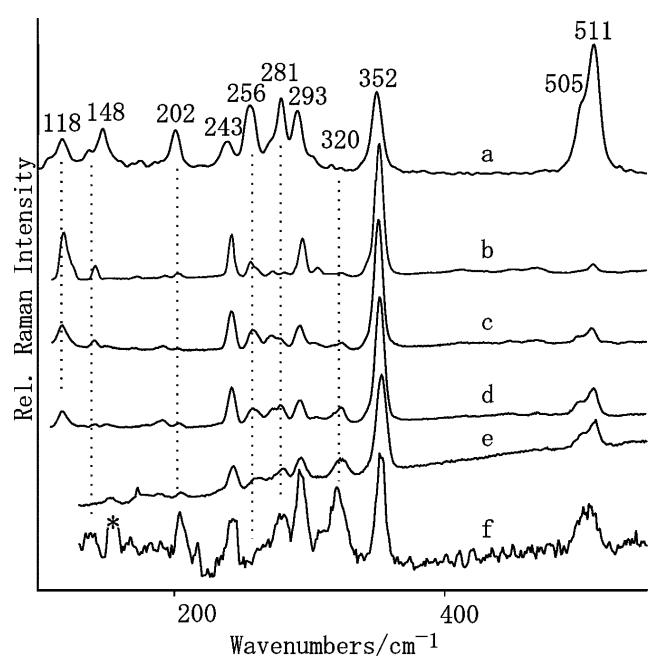

Fig. 4. Raman spectra of $K_2Ta_2S_{10}$, (a) FT-Raman, (b–f) resonance Raman, excitation line are 1064 nm (FT), 647, 568, 531, 515, and 455 nm, respectively.

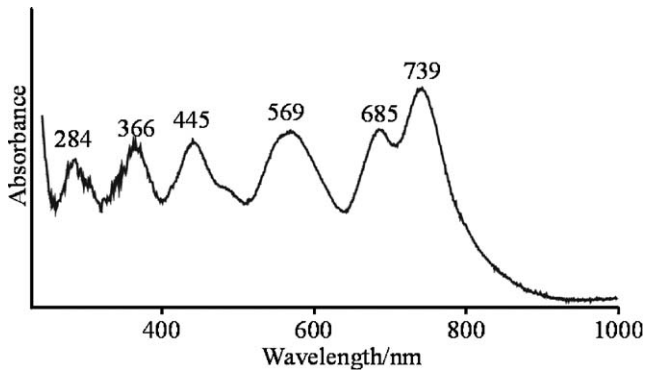

Fig. 5. UV/visible/near-IR spectrum of $K_2Ta_2S_{10}$.

"normal" or at best a pre-resonance Raman spectrum is observed (Fig. 4a). The S–S stretching vibration (ν(S–S)) at 511/505 cm^{-1} of the very polarisable disulfide ligands is the most intense Raman band as compared with the Ta–S stretching vibrations at 352, 320, 293, 281, 256, 243 cm^{-1} and the S–Ta–S deformation modes at 202, 148 and 118 cm^{-1} of the TaS_8 polyhedra. The assignment of ν(S–S) is sustained by the complementary infrared studies. According to the selection rules, no distinct absorption is detected around 500 cm^{-1}. The large hypsochromic shift of ν(S–S) of the coordinated disulfide ligands correlates well with the distinctly shorter S–S distance as compared with that of the disulfide ion, e.g. in K_2S_2 [30].

Applying excitations with higher energy Kr^+ and Ar^+ laser lines at 647.1, 568.2, 530, 514.5, and 454.7 nm (Fig. 4b–f), which are mainly only within the contour of the 569 nm electronic absorption band of the complex ion (Fig. 5), typical resonance Raman spectra are obtained. In coincidence of the excitation frequency with the maximum of this electronic absorption band, the resonance Raman spectrum in Fig. 4 is characterized by a significant enhancement of the intensity of the symmetric (Ta–S–Ta) stretching vibration (ν_1) of the (Ta–S–Ta) bridge at 352 cm^{-1}, and the appearance of an overtone progression reaching up to $3\nu_1$. On the other hand, all the bands of the other Ta–S vibrations and especially that of ν(S–S) of the disulfide ligand at 511/505 cm^{-1} show rather low intensities. In addition, all these low intense Ta–S vibrational modes form combinations with ν_1, but no subsidiary progressions with other possible Raman active Ta–S modes is observed. The bathochromic shift of the Ta–S vibrations correlates well with the longer Ta–S distances (shortest: 2.455(1) Å) compared to those (about 2.2 Å) found in the complex anions $[Ta_2S_{11}]^{4-}$ in $Tl_4[Ta_2S_{11}]$ [28] and t-$K_4[Ta_2S_{11}]$ [14] as well as in $TlTaS_3$ [29].

Interestingly, a further change of the signature of the resonance Raman spectrum starts to be discernible, when the excitation frequency approaches the electronic absorption band at 445 nm. From Fig. 4f, the intensity of ν_1 decreases, while the intensities of some lower energy Ta–S vibrational modes, especially that at 320 cm^{-1}, increase significantly. This observation indicates that this electronic absorption may be assigned to a S→Ta charge transfer of the Ta–S–S–Ta bridges, in contrast to the former electronic band at 569 nm involving mainly a S→Ta charge transfer of the Ta–S–Ta bridge. It is not surprising that because of the interfering Raman effects, the Raman spectra are incomplete, since only modes are enhanced which couple to the electronic transition in resonance. Hence, more complete excitation profiles including selected radiation within the contour of the other electronic absorption bands are necessary to better understand both the electronic absorption spectrum, that displays up to six distinct transitions at 739, 686, 569, 445, 366, and 284 nm, and the vibrational spectra of $K_2Ta_2S_{10}$.

In conclusion, a new one-dimensional compound $K_2Ta_2S_{10}$ containing TaS_8 polyhedra with disulfide anions in A/group5/Q (A = alkali metals; Q = chalcogen) system has been synthesized and characterized. The presence of one-dimensional chain anions in the compound obtained from a polychalcogenide flux suggests possible new phases formed by combinations of different building units of group 5 elements.

Attempts to prepare the analogous Rb and Cs compounds yielded the polysulfides $A_6Nb_4S_{22}$ (A = Rb, Cs) [18,19]. This observation suggests that the ionic radii of Rb^+ and Cs^+ are too large to stabilize the $[TaS_5]^-$ anionic chains.

Acknowledgment

Financial support by the state of Schleswig-Holstein is gratefully acknowledged.

References

[1] S.A. Sunshine, D. Kang, J.A. Ibers, J. Am. Chem. Soc. 109 (1987) 6202–6204.
[2] M.G. Kanatzidis, Chem. Mater. 2 (1990) 353–363.
[3] M.G. Kanatzidis, A.C. Sutorik, Prog. Inorg. Chem. 43 (1995) 151–265.
[4] P. Dürichen, W. Bensch, Eur. J. Solid State Inorg. Chem. 33 (1996) 309–320.
[5] M. Emirdag-Eanes, J.A. Ibers, Z. Kristallogr.–NCS 216 (2001) 489.
[6] M. Latroche, J.A. Ibers, Inorg. Chem. 29 (1990) 1503–1505.
[7] R. Niewa, G.V. Vajenine, F.J. DiSalvo, J. Solid State Chem. 139 (1998) 404–411.
[8] H. Yun, C.R. Randall, J.A. Ibers, J. Solid State Chem. 76 (1988) 109–114.
[9] O. Krause, C. Näther, I. Jess, W. Bensch, Acta Crystallogr. C 54 (1998) 902–904.
[10] W. Bensch, P. Dürichen, Eur. J. Solid State Inorg. Chem. 33 (1996) 527–536.
[11] W. Bensch, P. Dürichen, Inorg. Chim. Acta 261 (1997) 103–107.

[12] K.O. Klepp, G. Gabl, Z. Naturforsch. 53b (1998) 1236–1238.
[13] S. Schreiner, L. Aleandri, D. Kang, J.A. Ibers, Inorg. Chem. 28 (1989) 392–393.
[14] S. Herzog, C. Näther, W. Bensch, Z. Anorg. Allg. Chem. 625 (1999) 969–974.
[15] P. Dürichen, W. Bensch, Acta Crystallogr. C 54 (1998) 706–708.
[16] P. Stoll, C. Näther, W. Bensch, Z. Anorg. Allg. Chem. 628 (2002) 2489–2494.
[17] W. Bensch, P. Dürichen, Z. Anorg. Allg. Chem. 622 (1996) 1963–1967.
[18] P. Stoll, C. Näther, I. Jess, W. Bensch, Z. Anorg. Allg. Chem. 626 (2000) 959–962.
[19] P. Stoll, C. Näther, I. Jess, W. Bensch, Acta Crystallogr. C 56 (2000) e368–e369.
[20] P. Stoll, C. Näther, I. Jess, W. Bensch, Solid State Sci. 2 (2000) 563–568.
[21] M.A. Pell, G.V.M. Vajenine, J.A. Ibers, J. Am. Chem. Soc. 119 (1997) 5186–5192.
[22] P. Dürichen, M. Bolte, W. Bensch, J. Solid State Chem. 140 (1998) 97–102.
[23] O. Tougait, J.A. Ibers, Solid State Sci. 1 (1999) 523–534.
[24] W. Bensch, C. Näther, P. Dürichen, Angew. Chem. 110 (1998) 140–142.
[25] G.M. Sheldrick, SHELXS-97, Program for Crystal Structure Determination, University of Göttingen, Germany, 1997.
[26] G.M. Sheldrick, SHELXL-97, Program for Refinement of Crystal Structures, University of Göttingen, Germany, 1997.
[27] R.D. Shannon, Acta Crystallogr. A 32 (1976) 751–767.
[28] Ch.L. Teske, N. Lehnert, W. Bensch, Z. Anorg. Allg. Chem. 628 (2002) 2651–2655.
[29] Ch.L. Teske, W. Bensch, A. Perlov, H. Ebert, Z. Anorg. Allg. Chem. 628 (2002) 1511–1516.
[30] P. Böttcher, J. Getzschmann, R. Keller, Z. Anorg. Allg. Chem. 619 (1993) 476–488.